American Journal of Materials Science 2012, 2(4): 131-137
DOI: 10.5923/j.materials.20120204.06

Optical Properties of 3,4,9,10-Perylenetetracarboxylic Diimide (PTCDI) Organic Thin Films as a Function of Post-Annealing Temperatures

M. El-Nahhas[1], H. Abdel-Khalek[2], E. Salem[2,*]

[1]Physics department, Faculty of Education, Ain Shams University, Roxy 11757, Cairo, Egypt
[2]Physics Department, Faculty of Science, Suez Canal University, Ismailia, Egypt

Abstract In this work, effect of post-annealing on the structural and optical properties of thermally evaporated PTCDI films deposited on quartz substrates is reported. The optical properties were investigated using spectrophotometric measurements in wavelength range 200-2500 nm for as-deposited and annealed films with the same thickness at different temperatures. The XRD studies confirm the films have orthorhombic structure (PNA21) space group. The optical constants were accurately determined using reflectance and transmittance spectra. The dispersion of the refractive index is discussed in terms of single oscillator model. In addition, the ratio of free carrier concentration to its effective mass was estimated. The absorption analysis has been also performed in order to determine the type of electronic inter-band transitions for the films. Both direct and indirect transitions are present. The direct and indirect bandgap energy decreases with increasing temperature. The decrease in the energy can be explained by increase of delocalized π electrons due to thermal annealing.

Keywords Organic Thin Films, Optical Properties, Solar Cell

1. Introduction

A great increase in demand for low cost, high effect solar cell has intensified research into improving current technology and developing cutting-edge next generation photovoltaic devices. Today, most commercial solar cells are made from silicon. Like many conventional semiconductors, silicon offers excellent, well-established electronic properties. However, the use of silicon or other conventional semiconductors in photovoltaic devices has been limited by the high cost of production. The fabrication of even the simplest semiconductor cell is a complex process that has to take place under tightly controlled conditions, and for this reason researchers have long considered organic alternatives. Organic semiconductors can often be made a flexible, lightweight and inexpensive form of solar cells. The technology for these solar cells is progressing and they are gaining popularity due to their environmentally safe composition. Research into new technologies for the development of next generation photovoltaic has focused on the research and technical development of organic devices.

Extended and π-conjugated organic semiconductors have received much attention due to their excellent electronic performances. For example, the fluorescent dye 3,4,9,10-Perylenetetracarboxylic diimide or PTCDI is used extensively as an industrial pigment, because of its brilliant colour, strong absorption and fluorescence, and good thermal, chemical, and photochemical stability[1-4]. PTCDI and its derivatives are effective n-type organic semiconductors with various applications. For example, they are used as tunable laser dyes, light-harvesting materials, transistors, molecular switches, solar cells, and optoelectronic devices, such as light-emitting diodes, because of their unique optical and electrochemical properties[5-10]. There are indications that derivatives of perylenetetracarboxylic acid favour charge transfer due to large intermolecular coupling, and this may lead to the formation of charge transfer excitons[11,12].

Optical properties of active layer in solar cell are considered as trivial factor. Generally, it is believed that annealing can improve the crystallization and orientation of organic layer and influenced organic photovoltaic device efficiency significantly. Under thermal annealing processing, the refractive index (n) and extinction coefficient (k) of the active layer varies with distinct temperature. Through the optical constant variation, optical property of the multilayer system (solar cell) can be optimized. Therefore, Post-growth annealing has been proved to be an efficient approach to improve crystalline quality and optical properties of organic thin films. In this work, post-growth annealing was performed on 3,4,9,10-Perylenetetracarboxylic diimide thin films grown by thermal evaporation at room temperature. Ex

* Corresponding author:
eman_m_salem@yahoo.com (E. Salem)
Published online at http://journal.sapub.org/materials

situ optical spectroscopic measurements were performed to investigate the optical properties of annealed PTCDI thin films.

2. Experimental Details

Different PTCDI films with the same thickness of 400 nm were prepared by conventional thermal evaporation technique at a pressure of $p = 2\times10^{-4}$ Pa. Purified PTCDI powder (99.99% Sigma Aldrich Co.) was loaded into a molybdenum cell with nozzle of 5 mm in diameter on the top. The flat quartz substrates were located above 15 cm from the source. The substrates were carefully cleaned by putting them in chromic acid for 20 min and then they were washed several times with distilled water. After that the substrates were rinsed by isopropyl alcohol. The substrates were dried in a steam of dry nitrogen, and finally were cleaned by atomic bombardment in an initial stage of evacuation. The film thicknesses were controlled by using a quartz crystal thickness monitor and subsequently calibrated interferometrically by Tolansky's method[13]. All films were deposited at room temperature and the rate of deposition was 2.5 nm/s. After deposition, several films have been annealed at different temperatures under vacuum ($>10^{-1}$ Pa) for two hours.

Room temperature XRD measurements (X'Pert PRO Philips X-ray diffractometer) were carried out using $CuK_{\alpha 1}$ radiation in the ($\theta-2\theta$) geometry. The spectra of the films were scanned over the range of 5° to 90° (2θ), with a step rate of 0.02° (2θ) and a fixed counting time of 10s for each step, in order to obtain spectra with sufficient signal to noise ratio.

The transmittance $T(\lambda)$ and reflectance $R(\lambda)$ spectra of both as-deposited PTCDI and annealed films were measured at normal incidence at room temperature in the spectral range 200–2500 nm by using a computer-aided double-beam spectrophotometer (JASCO model V-570 UV–VIS-NIR). A blank quartz substrate was used as a reference for the transmittance scan.

In order to calculate the refractive index (n) and the absorption index (k) of the thin films at different wavelengths, the following equations were applied:

$$n = \frac{1+R}{1-R} + \sqrt{\frac{4R}{(1-R)^2} - k^2} \qquad (1)$$

and

$$\alpha = \frac{1}{d}\ln\left[\frac{(1-R)^2}{2T} + \sqrt{\frac{(1-R)^4}{4T^2} + R^2}\right] \qquad (2)$$

$$k = \frac{\alpha\lambda}{4\pi} \qquad (3)$$

where α is the absorption coefficient and d is the film thickness. The experimental error in measuring the film thickness was taken as ±2%, in T and R as ±1% and in the calculated values of n and k as 3% and 2.5%, respectively.

3. Results and Discussion

3.1. Structural Investigation

Figure 1 shows the X-ray diffraction (XRD) spectra of the powder, the as-deposited and the annealed PTCDI films. The CRYSFIRE & CHECKCELL computing programs[14,15] were used to index all the diffraction lines, calculate the Miller indices (hkl) and the interplanar spacing (d_{hkl}) value for each diffraction peak and finally to calculate the lattice parameters.

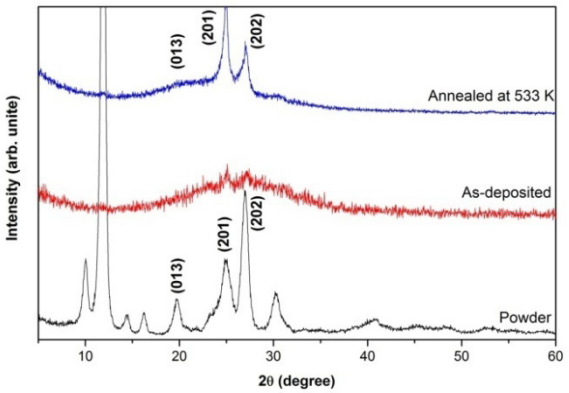

Figure 1. XRD spectra of 3, 4, 9, 10-perylene-tetracarboxylicacid-diimide, PTCDI in powder form and thin film as indicated in the figure

The analysis indicates that the films have orthorhombic structure (PNA21) space group with the following lattice parameters: $a = 7.368A^o$, $b = 10.924A^o$, $c = 14.777A^o$ and $\alpha = \beta = \gamma = 90^o$. Table 1 gives the values of Miller indices *hkl* for each diffraction peak, 2θ and the interplanar spacing (d_{hkl}) before and after refinement. These patterns also indicate that the as-deposited film is amorphous/nanocrystalline structure, while the annealed film is crystallized with (201) and (202) orientations.

Table 1. X-ray analysis for PTCDI powder

No.	$2\theta_{measured}$	$2\theta_{calculated}$	$d_{measured}$	$d_{calculad}$	I/I_o	*hkl*
1	10.0467	10.061	8.785	8.785	11.61	(011)
2	11.9631	11.968	7.3917	7.389	100	(002)
3	14.5169	14.489	6.0965	6.108	2.90	(110)
4	16.2116	16.214	5.4629	5.462	3.39	(020)
5	19.7454	19.755	4.49247	4.491	5.65	(013)
6	23.1524	23.178	3.83851	3.835	2.25	(113)
7	24.8825	24.888	3.5754	3.575	11.76	(201)
8	26.9704	26.998	3.30317	3.298	24.13	(202)
9	30.2900	30.271	2.9482	2.950	5.73	(203)
10	33.3223	33.433	2.6866	2.666	0.32	(115)
11	34.9576	34.958	2.5645	2.564	0.27	(042)
12	41.0664	41.066	2.19609	2.1961	1.08	(044)

3.2. Optical characterizations

The spectral behaviour of the transmittance, T and reflectance, R measured at normal incidence in a wavelength range 200–2500 nm for as-deposited and annealed PTDCI films of thickness 400 nm is shown in Fig. 2. It is quite clear that the intensities of transmittance within the absorption

region increase by annealing process. Also, the maximum reflectance intensity for as-deposited film and annealing temperature show that the reflectance intensities within the absorption region. In transparent region, ($\lambda > 1000$) all films have the same behaviour of T and R which indicate that the thickness does not change by annealing.

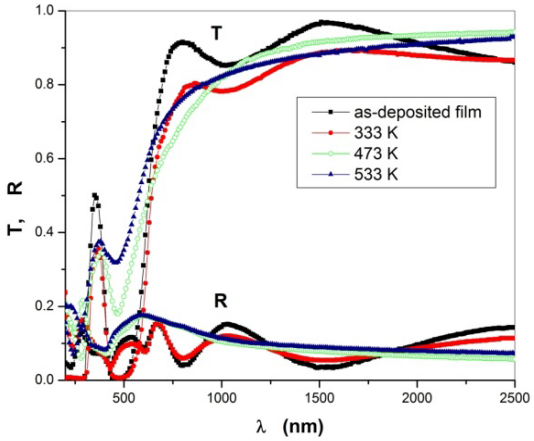

Figure 2. The spectral dependence of the transmittance, T and reflectance, R for as-deposited and annealed PTCDI films with thickness of 400 nm

The variation in the dispersion curve of the refractive index (n) for the as-deposited and the annealed PTCDI films are shown in Fig. 3.

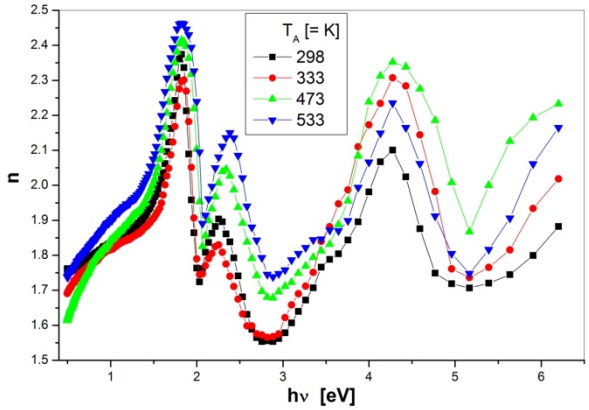

Figure 3. Spectral dependence of the real part of refractive index, n, for as-deposited and annealed PTCDI films

The spectral behaviour exhibits an anomalous dispersion in the range ($h\nu > 1.5$ eV) and a normal dispersion in the range ($h\nu < 1.5$ eV). At low photon energy, $h\nu \to 0$, the calculated value of real part of refractive index decreases by an amount of $\Delta n = 0.17$ after annealing at 533 K. In addition (Fig. 3) shows three peaks at 1.8, 2.2 and 4.3 eV. There are visible variations in the intensity of these peaks with a blue shift in the peak positions as a result of annealing. It is also found that the films with lower refractive index correspond to higher annealing temperature, leads to a decrease in mass density[16].

Figure 4 shows the variation of the imaginary part of the refractive index, extinction coefficient, k with photon energy for as-deposited and annealed PTCDI films. There are considerable differences in the intensity and in the position of the absorption peaks for the as-deposited and annealed films. It is clear that, there is a blue shift in the absorption edge and the intensity of the absorption peaks decreases with annealing temperature.

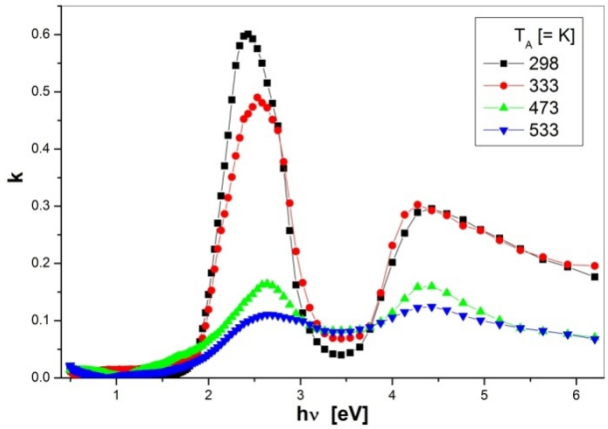

Figure 4. Spectral dependence of the imaginary part of refractive index, k, for as-deposited and annealed PTCDI films

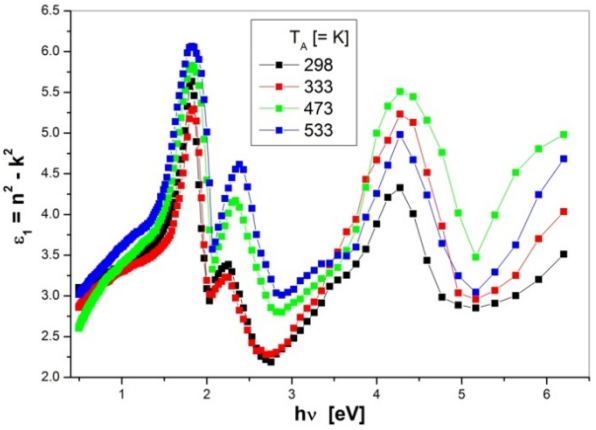

Figure 5. The variation of real part of complex dielectric constant with photon energy for as-deposited and annealed PTCDI films

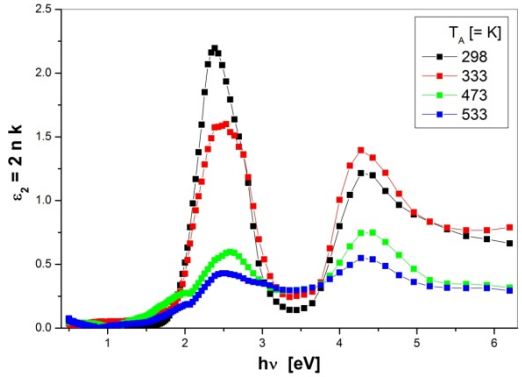

Figure 6. The variation of imaginary part of complex dielectric constant with photon energy for as-deposited and annealed PTCDI films

The complex dielectric constant, ε characterizes completely the propagation, reflection and loss of light in

thin film structure and provide important information about the electronic structure of materials. The complex dielectric constant is given by:

$$\varepsilon(h\nu) = \varepsilon_1(h\nu) - i\,\varepsilon_2(h\nu), \qquad \tan\delta = \frac{\varepsilon_2}{\varepsilon_1} \tag{4}$$

where $\varepsilon_1 = n^2 - k^2$ is the real part and $\varepsilon_2 = 2nk$ is the imaginary part of the complex dielectric constant, while $\tan\delta$ is the loss factor. Figures 5 and 6 show the real and imaginary parts of the complex dielectric constant, respectively. Hence, in the PTCDI films, the variation of ε_1 as a function of photon energy follows the same behaviour as n, whereas the variation of ε_2 follows the behaviour of k which is related to absorption coefficient α.

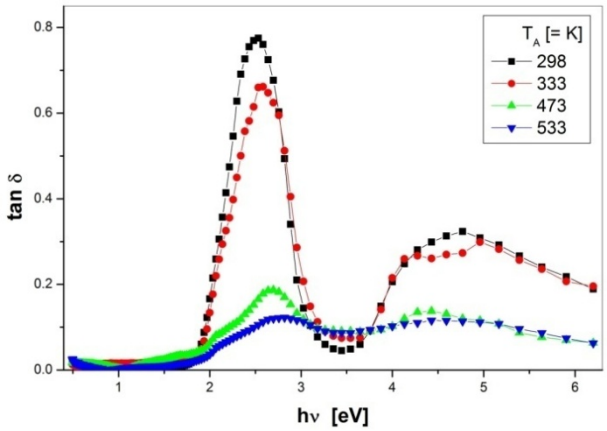

Figure 7. The variation in the loss factor with photon energy for the as-deposited and annealed PTCDI films

The variation in the loss factor, $\tan\delta$ with photon energy for the as-deposited and annealed PTCDI films is shown in Figure 7. The complex optical conductivity $\sigma^*(h\nu) = \sigma_1(h\nu) + i\,\sigma_2(h\nu)$ is related to the complex dielectric constant ε by the relation[17]:

$$\sigma_1 = \omega\varepsilon_2\varepsilon_o \qquad \sigma_2 = \omega\varepsilon_1\varepsilon_o \tag{5}$$

where ε_o is the permittivity of free space. The real σ_1 and imaginary σ_2 parts of the optical conductivity as a function of the photon energy are shown in Figures 8 and 9, respectively.

It is also possible to calculate the volume and surface energy loss functions (VELF and SELF) by using the relations[18]:

$$VELF = \left(\frac{\varepsilon_2^2}{\varepsilon_1^2 - \varepsilon_2^2}\right) \tag{6}$$

$$SELF = \frac{\varepsilon_2^2}{\left((\varepsilon_1+1)^2 + \varepsilon_2^2\right)} \tag{7}$$

The volume and the surface energy loss function as a function of the photon energy for the as-deposited and annealed PTCDI films are shown in Figures 10 and 11.

Generally, the dispersion behaviour can be modelled if it is assumed to be the response of a set of Lorentzian oscillators of adjustable strength and position[19]. Accordingly, the dispersion of refractive index has been analysed by applying the single oscillator model, in the normal dispersion region, and using the well known Wemple and DiDomenico equation[20,21]:

$$n^2 - 1 = \frac{E_d E}{E_o^2 - (h\nu)^2} \tag{8}$$

where E_o is the single oscillator energy (is related to the lowest direct gap) and E_d is the dispersion energy (is independent of both the absorption threshold (band gap) and the lattice constant)[20]. By plotting $(n^2-1)^{-1}$ versus $(h\nu)^2$ and fitting the data to a straight line, E_o and E_d can be determined from the intercept, E_o/E_d and the slope $-1/E_oE_d$.

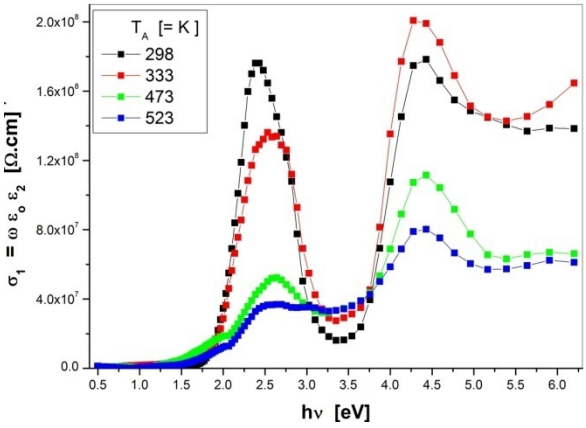

Figure 8. The variation of real part of optical conductivity with photon energy for as-deposited and annealed PTCDI films

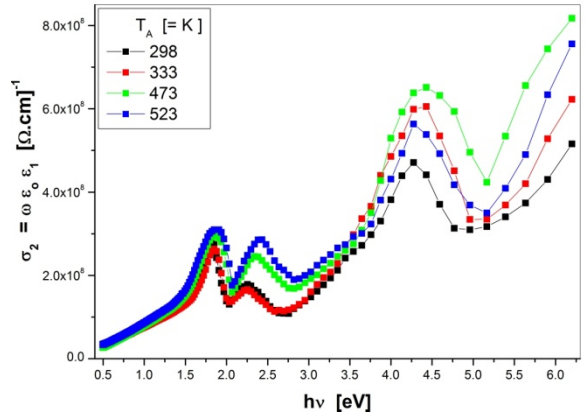

Figure 9. The variation of imaginary part of optical conductivity with photon energy for as-deposited and annealed PTCDI films

Another model equation that is widely used is given by[23]:

$$\varepsilon_1 = n^2 - k^2 = \varepsilon_L - \left(\frac{e^2}{4\pi^2 c^2 \varepsilon_o}\frac{N}{m^*}\right)\lambda^2 \tag{9}$$

where ε_L is the lattice dielectric constant, e is the elementary charge, c is speed of light and N/m* is the ratio of carrier concentration to the effective mass. The values of ε_L and (N/m*) are determined from the extrapolation of relation between n^2 and λ^2 to $\lambda^2 = 0$ and from the slope of the graph for the as-deposited and annealed PTDCI films and listed in Table 2.

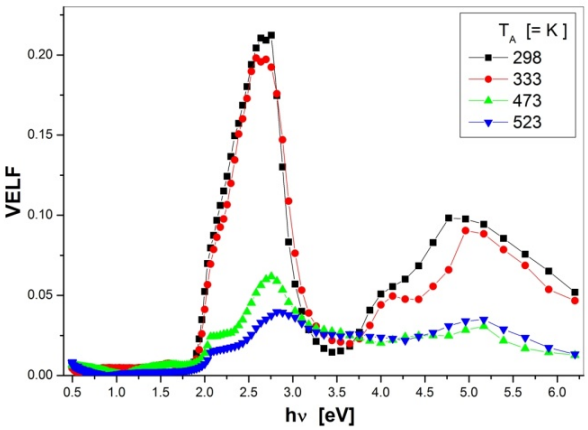

Figure 10. VELF as a function of photon energy for as-deposited and annealed PTCDI films

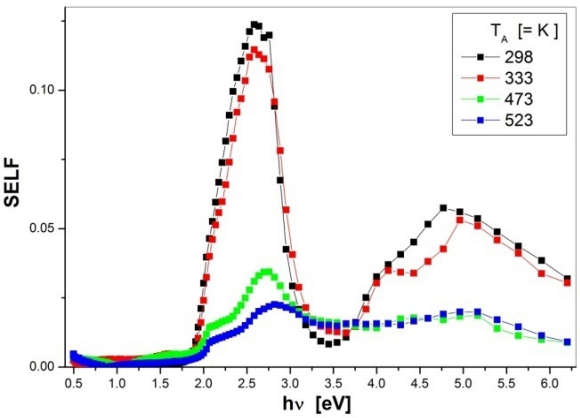

Figure 11. SELF as a function of photon energy for as-deposited and annealed PTCDI films

Table 2. Dispersion parameters of the PTDCI films

PTDCI	E_o (eV)	E_d (eV)	ε_L	N/m^* ($gm^{-1}\ cm^{-3}$)
As-deposited, 298 K	2.909	6.017	3.068	6.03×10^{46}
Annealed, 333 K	2.744	5.415	2.973	6.03×10^{46}
473 K	2.319	4.520	2.949	6.03×10^{46}
533 K	2.356	5.013	3.128	6.03×10^{46}

3.3. Optical Energy Gap

The spectral distribution of the absorption coefficient (α) for as-deposited and annealed PTCDI films are shown in Fig. 12. The dependence of the absorption coefficient on the photon energy is important to obtain information about the energy band structure and the type of optical transition. The general expression that relates the absorption coefficient to the energy band near absorption edge is given by[24]:

For allowed direct transitions

$$(\alpha h\nu) = A_d (h\nu - E_g^d)^{1/2} \quad (10)$$

For indirect allowed transitions

$$(\alpha h\nu) = A_{ind} (h\nu - E_g^{ind} \pm E_{phonon})^{1/2} \quad (11)$$

In the above equations, E_g^d and E_g^{ind} represent the band gap energy, while A_d and A_{ind} are characteristic constant parameters, independent of photon energy, for direct and indirect transition, respectively.

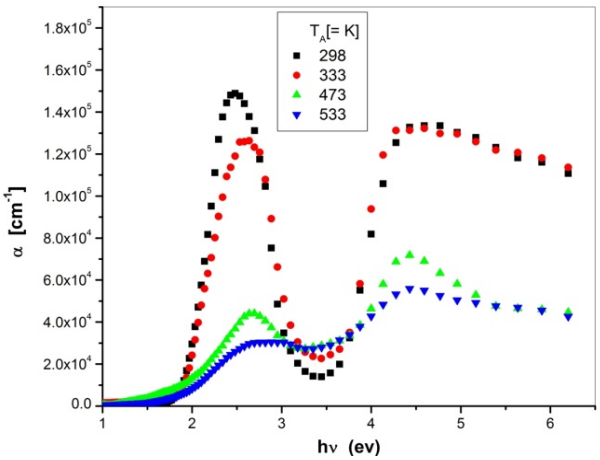

Figure 12. Spectral behaviour of the absorption coefficient for the as-deposited and annealed PTCDI films

Table 3. Values of energy gaps of as-deposited and annealed PTCDI films according to the band transition

PTCDI	E_{g1}^{ind} (eV)	E_{g2}^{ind} (eV)	E_{g1}^{d} (eV)
As-deposited, 298 K	1.76	3.30	3.81
Annealed, 333 K	1.71	3.44	3.81
473 K	1.52	3.07	3.75
533 K	1.57	2.78	3.57

Plots of $(\alpha h\nu)^2$ versus $(h\nu)$ (allowed direct transitions) and $(\alpha h\nu)^{1/2}$ versus $(h\nu)$ (allowed indirect transitions) for the as-deposited and annealed PTDCI films are shown in Figs. 13 and 14 respectively. The extrapolation of the straight line graphs to zero absorption gives the values of the energy gap and these values are listed in Table 3. In case of indirect transition there are two different transitions. The value of the indirect energy gap decrease by increasing the annealing temperature. On the other hand, there is only one transition for direct type of transition. The values of direct energy gap also decreases by increasing the annealing temperatures. The decrease in the energy gap can be explained because of the thermal annealing results in more delocalized π electrons, the lowering of the band gap between π and π *, and the increase of the optical π - π * transition which results in the observed red shift in the gap[25,26].

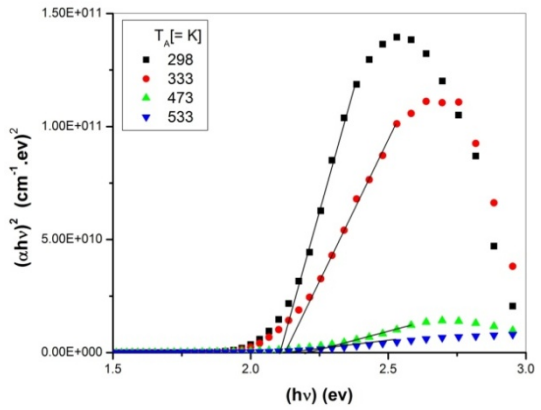

Figure 13. The plot of $(\alpha h\nu)^2$ versus the incident photo energy ($h\nu$) for as-deposited and annealed PTCDI films

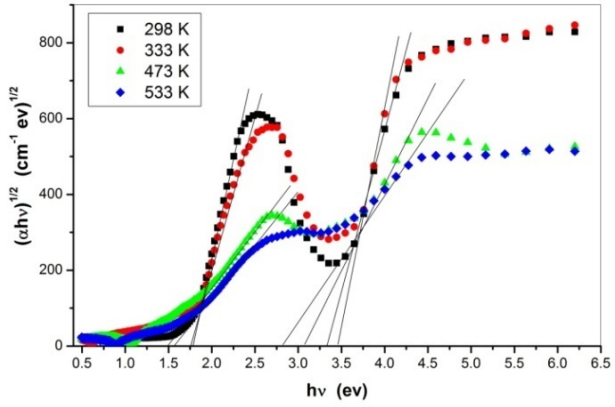

Figure 14. The plot of $(\alpha h\nu)^{1/2}$ versus the incident photo energy ($h\nu$) for as-deposited and annealed PTCDI films

4. Conclusions

Effects of post-annealing on the optical characterization of thermally evaporated PTCDI films have been carried out using spectrophotometric measurements. It was found that the refractive index of the as-deposited film increases with annealing. In addition, annealing affects the values of calculated dispersion parameters. The optical absorption spectra of the PTCDI film shows that the absorption spectra mechanism is due to both direct and indirect transition. The decrease in the energy gap can be explained because of the thermal annealing results in more delocalized π electrons, the lowering of the band gap between π and π *, and the increase of the optical π - π * transition which results in the observed red shift in the gap. All the results are self-consistent in the paper. This work would benefit the fabrication and investigation of organic solar cell and photovoltaic devices.

REFERENCES

[1] H. Zollinger, "Color chemistry: synthesis, properties and applications of organic dyes and pigments", 2nd ed. VCH Publisher, New York, 1991.

[2] J. Fabian, K. Zahradnik, "The search for highly colored organic compounds", Agew. Chem., Int. ed. Eng., vol.28, pp.677, 1989.

[3] H. Quante, Y. Geerts, K. Müllen, "synthesis of Soluble Perylenebisamidine Derivatives - Novel Long-wavelength Absorbing Dyes", Chem. Mater, vol.9, pp.495, 1997.

[4] L. Feiler, H. Langhals, K. Polborn, "Synthesis of perylene-3,4-dicarboximides-Novel highly photostable fluorescent dyes", Liebigs Ann, vol.7, pp.1229, 1995.

[5] S. K. Lee, Y. Zu, A. Herrmann, Y. Geerts, K. Müllen, A. J. Bard, "Electrochemistry, Spectroscopy and Electrogenerated Chemiluminescence of Perylene, Terrylene, and Quaterrylene Diimides in Aprotic Solution", J. Am. Chem. Soc, vol.121, pp.3513, 1999.

[6] J. Choi, W. Lee, C. Sakong, S. B. Yuk, J. S. Park, J. P. Kim, "Facile synthesis and characterization of novel coronene chromophores and their application to LCD color filter", Dyes Pigments, vol.94, pp.34, 2012.

[7] B. A. Gregg, "Photovoltaic properties of a molecular semiconductor modulated by an exciton-dissociating film", Appl. Phys. Lett, vol.67, pp.1271, 1995.

[8] C. G. Claessens, U. Hahn, T Torres, "Phthalocyanines: From outstanding Electronic Properties to Emerging Applications", The Chemical Record, vol.8, pp.5, 2008.

[9] M. P. O'Neil, M. P. Niemczyk, W. A. Svec, D. Gosztola, G. L. Gaines, M. R. Wasielewski, "Picosecond Optical Switching Based on Biphotonic Excitation of an Electron Donor-Acceptor-Donor Molecule", Science, vol.257, pp.63, 1992.

[10] S. Tasch, E. J. W. List, O. Ekström, W. Graupner, G. Leising, P. Schlichting, U. Rohr, Y. Geerts, U. Scherf, K. Müllen, "Efficient white light-emitting diodes realized with new processable blends of conjugated polymers", Appl. Phys. Lett, vol.71, pp.2883, 1997.

[11] G. Mazur, P. Petelenz, M. Slawik, "Theoretical calculations of the electroabsorption spectra of perylenetetracarboxylic dianhydride", J. Chem. Phys, vol.118, pp.1423, 2003.

[12] V.J. Sapagovas, V. Gaidelis, V. Kovalevskij, A. Undzenas, "3,4,9,10-Perylenetetracarboxylic acid derivatives and their photophysical properties", Dyes Pigments, vol.71, pp.178, 2006.

[13] D. S. Kumar, Y. Yoshida, "Dielectric properties of plasma polymerized pyrrole thin film capacitors", Surf. Coat. Tech, vol.169, pp.600, 2003.

[14] R. Shirley, "The CRYSFIRE System for Automatic Powder Indexing: User's Manual", The Lattice Press, Guildford, Surrey GU2 7NL, England, 2000.

[15] J. Laugier, B. Bochu, LMGP-Suite of Programs for the interpretation of X-ray Experiments, ENSP/Laboratoire des Matèriaux et du Gènie Physique, Saint-Martind'Hères, France, vol.46, pp.38042, 2000.

[16] B. Andreas, I. Breunig, K. Buse, "Modeling of X-ray-Induced Refractive Index Changes in Poly(methyl methacrylate)", Chem. Phys. Chem, vol.6, pp.1, 2005.

[17] F. Yakuphanoglu, M. Sekerci, O. F. Ozturk, "The determination of the optical constants of Cu(II) compound having 1-chloro-2,3-o-cyclohexylidinepropane thin film", Opt. Commun, vol.239, pp.275, 2004.

[18] J. I. Pankove, "Optical processes in semiconductors", New York: Dover publication institute, 1971.

[19] M. G. Krishna, J.S. Pillier, A.K. Bhattacharya, "Variable optical absorption edge in ion beam sputtered thin ytterbium oxide films", Thin Solid Films, vol.375, pp.218, 1999.

[20] S. H. Wemple, M. DiDomenico, "Optical Dispersion and the Structure of Solids", Phys. Rev. Lett, vol.23, pp.1156, 1969.

[21] S. H. Wemple, M. DiDomenico, "Behavior of the Electronic Dielectric Constant in Covalent and Ionic Materials", Phys. Rev. B, vol.3, pp.1338, 1971.

[22] N. K. Sahoo, K. V. S. R. Apparao, "Process-parameter optimization of Sb2O3 films in the ultraviolet and visible region for interferometric applications", Appl. Phys. A, vol.63. pp.195, 1996.

[23] P. O. Edward, "Handbook of optical constants of solids", Academic Press, New York, 1985.

[24] U. Pal, D. Samanta, S. Ghori, A.K. Chaudhuri, "Optical constants of vacuum-evaporated polycrystalline cadmium selenide thin films", J. Appl. Phys, vol.74, pp.6368, 1993.

[25] G. Li, V. Shrotriya, Y. Yao, Y. Yang, "Investigation of annealing effects and film thickness dependence of polymer solar cells based on poly(3-hexylthiophene)", J. Appl. Phys, vol.98, pp.043704, 2005.

[26] M. M. El-Nahass, A. F. El-Deeb, H. S. Metwally, A. M. Hassanien, "Influence of annealing on the optical properties of 5,10,15,20-tetraphenyl-21H, 23H-porphine iron (III) chloride thin films", Mater. Chem. Phys, vol.125, pp.247, 2011